Copper Tolerance of *Listeria monocytogenes* strain DRDC8

Francesca Y Bell, B. Biotech. (Hons.) (Adelaide)

A thesis submitted for the Degree of Doctor of Philosophy

School of Molecular and Biomedical Science
Faculty of Sciences,
The University of Adelaide
Adelaide, South Australia, Australia

May, 2010

Chapter 4: Mutagenesis of Genes implicated in Copper Ion Tolerance

4.1 Introduction

Copper homeostasis mechanisms involving proteins encoded on plasmids in Gram-positive bacteria have been previously described (Hasman, 2005; Liu *et al.*, 2002). These typically comprise membrane bound proteins involved in copper ion influx and/or efflux that interact with accessory proteins. The function of known accessory proteins includes regulation of copper homeostasis, copper binding/sequestration and protection of the cell from copper mediated damage. Similarly, it is clear that the dairy isolate *L. monocytogenes* strain DRDC8 carries a cluster of plasmid-encoded ORFs (pCT0017, pCT0018, pCT0019, pCT0020, pCT0023, pCT0024, pCT0025, pCT0026 and pCT0027) that may encode proteins involved in copper ion homeostasis (This thesis; Francis, 1996; Bell, 2002). Based on predictions of function and proximity to the *ctpA* gene (pCT0020), ORFs pCT0017, pCT0018 and pCT0019 are likely to comprise a set of accessory genes involved in *ctpA*-mediated copper ion transport. Even though no data is available to indicate that ORFs pCT0017, pCT0018, pCT0019 together with *ctpA* are cotranscribed, they may represent a *cop*-like operon within this larger gene cluster.

The polypeptide sequence encoded by ORF pCT0017 shares significant similarity to CopY-like negative repressor proteins that are involved in regulation of expression of *cop*-like operons (Bell, 2002). pCT0017 protein shares significant similarity to the CopY negative regulatory protein that controls expression of the well-characterized *cop* operon of *E. hirae* (Strausak & Solioz, 1997). It is possible that this protein controls expression of *ctpA* and cotranscribed genes eg. pCT0017, pCT0018, pCT0019 and *ctpA* (Bell, 2002). Similarly, sequence analysis has shown that pCT0018 and pCT0019 may encode accessory proteins involved in *ctpA* mediated copper ion transport (Bell, 2002). In particular, as CtpA apparently lacks an N-terminal cation binding motif (Bell, 2002; Francis & Thomas, 1997a), a copper binding motif may be located on a separate, but interacting protein. Indeed, ORF pCT0018 encodes a putative C-terminal CXMXMXH metal binding motif that may be involved in binding copper ions (Dancis *et al.*, 1994; Puig & Thiele, 2002).

In addition to *ctpA*, a chromosomal ORF (*cutR*) was identified as a gene that may encode a copper-translocating P-type ATPase that is also involved in copper ion homeostasis in *L. monocytogenes* strain DRDC8. The deduced polypeptide sequence of this ORF shares significant similarity with chromosomally-encoded copper-translocating P-type ATPases of other *Listeria* strains. The possibility that copper homeostasis in this strain involves both chromosomal and plasmid-encoded proteins is not novel and has been previously described in other bacterial species (reviewed by Cooksey, (1994); and Silver, (1998)). Proteins encoded by chromosomal (*cutR*) and plasmid (*ctpA* and associated ORFs) genes may be required to maintain copper ion homeostasis in the presence of high copper levels. CutR and CtpA-dependent copper translocation may act in synergy, or these systems may function autonomously.

Against this background, the aim of the work described in this chapter was to provide evidence to show that ORFs pCT0017, pCT0018, pCT0019 and *cutR* are involved in copper ion tolerance. This was achieved by analysis of the effects of independent mutations (pCT0017::*erm,* pCT0018::*erm*, pCT0019::*erm* or *cutR*::*erm*) on the ability of *L. monocytogenes* to tolerate copper ion stress. The impact of loss of plasmid pCT100 on copper tolerance by DRDC8 and a *cutR*::*erm* variant was also examined.

4.2 Experimental design

To determine whether ORFs pCT0017, pCT0018, pCT0019 and *cutR* play a role in copper tolerance, *erm* insertion mutations were created in each of these ORFs. The mobilisable suicide vector pKSV7 was used to construct allelic replacement mutations in pCT0017::*erm,* pCT0018::*erm*, pCT0019::*erm* and *cutR*::*erm* variants of *L. monocytogenes* strain DRDC8. Furthermore, DRDC8 and the *cutR*::*erm* mutant strain DSE955 were cured of plasmid DNA to assess the loss of plasmid-encoded genes on copper tolerance and the interdependence of *cutR* and *ctpA*. The ability of *L. monocytogenes* strains to tolerate copper ion stress was determined by measuring the minimal inhibitory concentrations of copper sulphate, as well as studying the effect of copper sulphate on growth. Minimal inhibitory concentration experiments were also used to determine if these independent mutations or loss of plasmid DNA impact on the ability of *L. monocytogenes* to transport

of other cations such as cadmium. Insertion mutants and plasmid-cured variants were prepared as follows.

1. Overlap extension PCR was used to first introduce a *Bam*HI restriction site within the ORF of interest, followed by insertion of a 1136 bp *Bam*HI DNA fragment that encoded an erythromycin resistance (*erm*) gene. Insertion mutation constructs were cloned into the suicide vector pKSV7. Confirmed constructs were then introduced into *L. monocytogenes* strain DRDC8 by electroporation and putative mutants selected following allelic replacement. Each allelic replacement mutant was then confirmed by PCR, sequence analysis and Southern hybridization analysis.
2. Plasmid-cured variants of *L. monocytogenes* strain DRDC8 were prepared by acridine orange treatment. Loss of plasmid DNA was confirmed by PCR analysis.

4.3 Results

4.3.1 Construction of *erm* Insertion Mutations

Overlap extension PCR was used to introduce a *Bam*HI restriction site via nucleotide changes into ORFs pCT0017, pCT0018, pCT0019 and *cutR*. The strategy used is shown diagrammatically in Figure 4.1. Oligonucleotide pairs MokBR/MokBF, FBEBF/FBEBR, FBDBF/FBDBR, and CuBamF/CuBamR were designed to amplify DNA regions containing 'nearly' *Bam*HI sites within these ORFs to introduce nucleotide base changes to encode a *Bam*HI site (GGATCC). Oligonucleotide pairs were also designed to amplify overlapping DNA fragments from each ORF using DNA extracted from *L. monocytogenes* strain DRDC8 (Section 2.7.2, Method 2). The MokFF/MokBR and MokFR/MokBF oligonucleotide pairs amplified 353 bp and 495 bp regions containing fragments of pCT0017; the FBdef/FBEBR and p1037/FBEBF pairs amplified 509 bp and 524 bp regions containing fragments of pCT0018; the FBdef/FBDBR and p1037/FBDBF pairs amplified 675 bp and 358 bp regions containing fragments of pCT0019; and the CuTrF/CuBamR and CuBamF/CuMutR pairs amplified 672 bp and 615 bp regions within *cutR* (see Table 2.7 for oligonucleotide description). PCR amplification of each fragment was confirmed by gel electrophoresis and sequence analysis following purification. These PCR reactions introduced a *Bam*HI site in overlapping regions for each pair of amplicons.

The overlapping DNA fragments of each ORF were combined in equal concentrations, denatured by heating at 95°C, and rapidly cooled to allow formation of overlapping DNA hybrids representing fragments of each ORF. Hybrids were used as template DNA for PCR amplification of 830 bp, 1003 bp, 1003 bp, and 1250 bp fragments using the MokFF/MokFR (pCT0017), p1037/FBdef (pCT0018), p1037/FBdef (pCT0019), and CuMutR/CuTrF (*cutR*) oligonucleotide pairs, respectively. Introduction of the *Bam*HI site was confirmed by restriction enzyme digestion and sequence analysis following purification of the PCR product (see Appendix F page 330, Appendix G page 331, Appendix H page 332, and Appendix I page 333, for nucleotide and deduced amino acid sequence).

The strategy used to construct *erm* insertion mutations in pCT0017, pCT0018, pCT0019 and *cutR* is shown diagrammatically in Figure 4.2. PCR products representative of pCT0017, pCT0018, pCT0019 and *cutR* containing introduced *Bam*HI sites were cloned into pGEM®-T Easy (see Table 2.3) to create plasmids pCT750, pCT751, pCT752 and pCT755, respectively. The resulting plasmid DNA was then used to chemically transform competent *E. coli* strain DH5α (refer to Table 2.2). Transformants were plated on LA containing Amp, IPTG and X-gal and incubated overnight at 37°C. White, *lac* negative colonies were selected. Plasmid DNA was isolated and clones carrying the correct insert were identified using *Eco*RI and *Bam*HI restriction endonuclease digestion analysis (see Figure 4.3) and sequence analysis.

A 1136 bp *Bam*HI fragment encoding an erythromycin resistance cartridge (*erm*) was isolated from plasmid pCT800[18] (refer to Table 2.3) and purified by agarose gel electrophoresis. The *Bam*HI *erm* fragment was ligated with similarly digested plasmids pCT750, pCT751, pCT752 and pCT755 to create plasmids pCT850, pCT851, pCT852 and pCT855, respectively. Clones carrying the correct *erm* insert were identified using restriction enzyme digestion analysis. These clones carried the expected 1966, 2139, 2139 and 2386 bp *Eco*RI fragments of the cloned fragments of ORFs pCT0017, pCT0018, pCT0019 and *cutR*, respectively, mutated by insertion of the 1136 bp *erm* fragment. In addition, each clone contained the expected 1136 bp *Bam*HI fragment (data not shown).

Further confirmation of these constructs was obtained by sequence analysis. This was also used to determine the orientation of the *erm* cassette with respect to the open reading frame.

4.3.2 Construction of *L. monocytogenes* Allelic Replacement Mutants

Plasmid pKSV7 (refer to Table 2.3) is a shuttle vector capable of replication in *E. coli* and temperature-sensitive replication[19] in Gram-positive bacteria including *L. monocytogenes* (Smith & Youngman, 1992). pKSV7 was used to mediate allelic replacement mutagenesis of wild type pCT0017, pCT0018, pCT0019 and *cutR* in *L. monocytogenes* strain DRDC8. Figure 4.4 represents the experimental strategy employed.

*Eco*RI DNA fragments carrying pCT0017::*erm*, pCT0018::*erm*, pCT0019::*erm* and *cutR*::*erm* were isolated from plasmids pCT850, pCT851, pCT852 and pCT855 by *Eco*RI digestion (refer to Section 4.3.1, Figure 4.2). Each fragment was then cloned into *Eco*RI digested pKSV7 to create plasmids pKS950, pKS951, pKS952 and pKS955, respectively. The resulting plasmid DNA was used to chemically transform competent *E. coli* DH5α cells. Transformants were plated on LA containing Amp, IPTG and X-gal and incubated overnight at 37°C. White, *lac* negative colonies were selected. Plasmid DNA was isolated and clones carrying the correct insert were identified using *Eco*RI and *Bam*HI restriction endonuclease digestion analysis and sequence analysis as described in Section 4.3.1.

Insertion mutations in ORFs pCT0017, pCT0018, pCT0019 and *cutR* cloned as plasmids pKS950, pKS951, pKS952 and pKS955 respectively, were introduced into a Sm resistant variant of *L. monocytogenes* (strain DRDC8Sm*)[20] by electro-transformation (refer to methods described in Section 2.10). Transformants were selected on BHI containing Sm and Cm.

---

[18] This *Bam*HI fragment was originally isolated from plasmid pGI21 (Table 2.3). This plasmid carries the *ermR* gene of plasmid pAMβ1. The nucleotide sequence of this 1136 *erm* fragment is shown in Appendix J.

[19] Temperature-sensitive replication functions derived from pE194ts

[20] *L. monocytogenes* DRDC8Sm* is a spontaneous Sm resistant variant of DRDC8 generated by plating strain DRDC8 on BHI agar containing 200 μg mL^{-1} Sm. To ensure that DRDC8Sm* was a variant of *L. monocytogenes* capable of infecting mammalian cells, the strain was maintained by serial passage through J774 cell monolayers (see Section 2.21).

The principle of allelic exchange provided a mechanism by which wild type alleles were replaced by mutated genes carried on the pKSV7 derived plasmids. To select for allelic exchange mutants, the cloned mutations were integrated into homologous regions of the DRDC8 genome by three consecutive rounds of overnight culture at the restrictive temperature of 40°C in 10 mL BHI broth in the presence of Cm (10 μg ml^{-1}). These strains were then subject to five consecutive rounds of culture at the permissive temperature of 30°C without Cm to facilitate allelic exchange. This was followed by curing of the excised pKSV7 derived plasmid through three sequential subcultures at 40°C. Putative allelic exchange mutants (Cm^S, Em^R, Sm^R) were identified by loss of Cm resistance through replica patching single Em^R, Sm^R colonies onto BHI agar containing Em, Sm and Cm.

Putative mutant strains containing the *cutR*::*erm* mutation (strain DSE955), the pCT0017::*erm* mutation (strain DSE950), the pCT0018::*erm* mutation (strain DSE951) and the pCT0019::*erm* mutation (strain DSE952) were selected for confirmation of allelic exchange mutation by PCR and Southern hybridisation analysis (Section 4.3.3).

4.3.3 Confirmation of Allelic Replacement Mutants

PCR amplification of chromosomal marker DNA (*hly* and *cutR* (refer to Table 2.9 for oligonucleotides used) from DNA extracted from putative mutant strains DSE950 (pCT0017::*erm*), DSE951 (pCT0018::*erm*), DSE952 (pCT0019::*erm*) and DSE955 (*cutR*::*erm*) was used to confirm that these strains were derived from the DRDC8Sm* background (refer to Appendix K, page 336 for supporting results). Loss of the pKSV7 derived chloramphenicol resistance (*cat*) gene was confirmed by PCR analysis using the catPF/catPR oligonucleotide pair (refer to Table 2.9). No amplicons were detected for any of the putative mutant strains, while a 391 bp region of the gene was amplified from control DNA prepared from *L. monocytogenes* cultures containing integrated copies of pKS950, pKS951, pKS952 and pKS955 [21] (see Appendix K, page 336).

[21] *L. monocytogenes* strain DRDC8Sm* carrying pKS950, pKS951, pKS952 or pKS955 grown at 40°C in the presence of Cm (10 μg mL^{-1}) for three consecutive rounds of subculture, see Section 4.3.2.

PCR analysis of DNA extracted from the putative mutant strains DSE950, DSE951, DSE952 and DSE955 was conducted using specific oligonucleotide combinations to confirm the presence of an *erm* insertion mutation in the respective genes. For each mutant, internal *erm*-specific primers (ermF2 and ermR2 (refer to Table 2.7 for oligonucleotide description)), designed to prime extension out of the *erm* gene, were used in combination with primers that flanked the site of allelic replacement. The ermF/ermR oligonucleotide pair was also used to confirm the presence of the *erm* gene in some of these strains by amplification of a 645 bp internal fragment of the gene. Southern hybridisation analysis of *Dra*I and *Eco*RV digested DNA was used to confirm the PCR data. A DIG labelled 645 bp internal *erm* fragment, amplified by PCR from plasmid pCT800 using the ermF/ermR oligonucleotide pair, was used as a DNA probe. DNA extracted from *ctpA*::*erm* strain DSE201 was included in each analysis as a positive control[22]. The respective pKSV7 based vector (ie. pKS950, pKS951, pKS952 or pKS955) and DNA extracted from the corresponding *L. monocytogenes* strain carrying the integrated plasmid (ie. pKS950 co-integrate, pKS951 co-integrate, pKS952 co-integrate or pKS955 co-integrate) were also included in each analysis as positive controls[23]. *Bam*HI digested plasmid pCT800 was included as an additional positive control, where probe DNA was expected to hybridise to a 1136 bp fragment carrying *erm*.

4.3.3.1 Characterisation of DSE950, a Putative pCT0017::*erm* Strain

DNA extracted from the putative pCT0017::*erm* mutant strain DSE950, was initially analysed by PCR using the FB1865/p2037, FB1865/ermR2, p2037/ermF2 and ermF/ermR oligonucleotide pair combinations (refer to Table 2.7 for oligonucleotide description). These primer combinations were used based on the orientation of the *erm* insertion within pCT0017 (as previously determined in Section 4.3.1). Oligonucleotides FB1865 and p2037 were designed to flank the DNA region targeted for exchange. Figure 4.5 presents data that showed that a 1496 bp PCR product, indicative of insertion of the 1136 bp *erm*

[22] The DSE201 DNA fragments that the *erm*-specific probe DNA would hybridise with was calculated from on the known location and orientation of the *erm* insertion in the 5' end of the *ctpA* gene.
[23] The size of the DNA fragment that probe DNA would hybridise with was calculated from the known plasmid sequence.

gene into pCT0017, was obtained using the p2037/ermF2 oligonucleotide pair. Similarly, amplification of a 645 bp product from DSE950 DNA using the ermF/ermR oligonucleotide pair confirmed that the *erm* gene was present. However, PCR products could not be amplified using the FB1865/ermR2 or FB1865/p2037 oligonucleotide pairs. Whilst sequence analysis confirmed that the PCR product amplified by the p2037/ermF2 (1496 bp) primer pair was indicative of successful allelic exchange (refer to Appendix L, page 338 for relevant sequence data), amplicons 1011 bp (for the FB1865/ermR2 primer pair) and 2859 bp (for the FB1865/p2037 primer pair) in size should have been amplified if the strain contained a *erm* insertion mutation in pCT0017.

Further PCR analysis showed that while the expected 2219 bp fragment (1136 bp *erm* fragment in addition to the 1083 bp product amplified from the positive control strain DRDC8Sm*) was amplified from DSE950 DNA using the MokFF/FB003 oligonucleotide pair, upstream DNA (5') was not amplified using the FB1863/S12210 oligonucleotide pair (refer to Table 2.7 for description) (Figure 4.6). Conversely, the data presented in Figure 4.6 shows that a 1427 bp product was amplified from strain DRDC8Sm* using the same primer pair. These observations were consistent with the PCR data shown in Figure 4.5. Collectively this experimental evidence indicated that while the pCT0017::*erm* DNA carried on plasmid pKS950 was integrated into the DSE950 DNA, this strain contained an insertion that resulted from excision/rearrangement of both target and vector DNA.

This conclusion was confirmed by Southern hybridisation analysis. The data presented in Figure 4.7 showed that while *erm*-specific probe DNA hybridised to one *Dra*I DSE950 DNA fragment of the expected size (1215 bp), probe DNA also hybridised to *Dra*I (*ca*. 1718 bp) and *Eco*RV (*ca*. 6900 bp) fragments not consistent with allelic exchange of the 1136 bp *erm* insertion in pCT0017. If strain DSE50 was a pCT0017::*erm* mutant, probe DNA should have hybridised with *Dra*I fragments 1215 bp and 956 bp in size, and an *Eco*RV fragment 7273 bp in size. The data presented in Figure 4.7 also showed that the expected results were obtained for all negative and positive controls: probe DNA did not hybridise with DRDC8Sm* DNA; probe DNA hybridised to two *Dra*I (1014 bp and 3347 bp) and an *Eco*RV fragment (7273 bp) from strain DSE201, two *Dra*I (*ca*. 1215 bp and 1718 bp) and an *Eco*RV fragment (*ca*. 8995 bp) from strain pKS950 co-integrate and plasmid pKS950, and a 1136 bp *Bam*HI fragment from plasmid pCT800. Together with

the PCR results described above, this data indicated that during allelic exchange, a partial resolution of integrated pKS950 lead to an unexpected excision/rearrangement in strain DSE950.

As it is unlikely that strain DSE950 contained the pCT0017::*erm* mutation, an additional 25 Cm^S, Em^R and Sm^R putative pCT0017::*erm* mutants were selected and each screened for the presence of the *erm* insertion mutation. These strains were analysed by PCR using the FB1865/p2037, FB1865/ermR2, p2037/ermF2 and ermF/ermR primer pair combinations. PCR products of the predicted size were amplified from DNA extracted from all 25 putative mutants using the p2037/ermF2 (1496 bp) and ermF/ermR (645 bp) oligonucleotide pairs, but amplicons were not produced for the FB1865/ermR2 or FB1865/p2037 primer pairs (refer to Appendix M, page 339 for PCR analysis of 5 of these putative mutants). This indicated that, like strain DSE950, complete allelic replacement had not been achieved in any of these strains. Southern hybridisation analysis of DNA extracted from these 25 isolates confirmed these results. Labelled *erm* DNA hybridised to two *Dra*I (*ca*. 1215 bp and 1718 bp) and a single *Eco*RV DNA fragment (from *ca*. 6900 to 8600 bp in size) for all 25 isolates (refer to Appendix N, page 341 for the Southern hybridisation results obtained for 7 of these putative mutants). This data indicated that like strain DSE950, the Cm^S, Em^R and Sm^R phenotype of these isolates was likely to be the result of partial resolution during allelic exchange resulting in excision of both target and vector DNA. As these putative mutants were atypical, they were not further analysed. Given that typical pCT0017::*erm* mutants could not be isolated, it was concluded that construction of a pCT0017::*erm* mutant would not be further explored. Possible reasons for this outcome are discussed in Section 4.4.

4.3.3.2 Characterisation of pCT0018::*erm* strain DSE951 and pCT0019::*erm* strain DSE952

To provide evidence to show that strains DSE951 and DSE952 carry pCT0018::*erm* and pCT0019::*erm* insertion mutations, respectively, PCR analysis was conducted using oligonucleotide pairs FB1865/p2037, FB1865/ermF2, p2037/ermR2 and ermF/ermR. These primer combinations were used based on the orientation of the *erm* insertion within pCT0018 and pCT0019 (as previously determined in Section 4.3.1). Oligonucleotides

FB1865 and p2037 were designed to flank the DNA fragment targeted for exchange in both strains. PCR analysis conducted using these primer pairs allowed amplification of products indicative of successful allelic replacement for both strain DSE951 and DSE952 (Figure 4.8 Panel A). Products 1345 bp and 1162 bp in size were amplified from DSE951 DNA using the FB1865/ermF2 and p2037/ermR2 oligonucleotide pairs, respectively. Similarly, these primer pairs allowed amplification of PCR products 1511 bp (FB1865/ermF2) and 996 bp (p2037/ermR2) in size from DSE952 DNA. In addition, PCR products indicative of amplification of a 645 bp internal fragment of the *erm* gene were produced from both DSE951 and DSE952 DNA using the ermF/ermR oligonucleotide pair (Figure 4.8 Panel B). The data presented in Figure 4.8 Panel B also shows that PCR products of the expected size (2859 bp) were amplified from both DSE951 and DSE952 DNA using the FB1865/p2037 oligonucleotide pair. The difference in fragment size amplified using this primer pair for strain DRDC8Sm* (1723 bp) compared to that obtained for DSE951 and DSE952 (2859 bp), is consistent with insertion of the 1136 bp *erm* gene in pCT0018 and pCT0019, respectively. This was further confirmed by sequence analysis (refer to Appendix O, page 342 and Appendix P, page 344).

Southern hybridisation analysis of *Dra*I and *Eco*RV digested DNA from DSE951 provided confirmatory data to show that this strain is a pCT0018::*erm* mutant. Probe DNA hybridised to two *Dra*I DSE951 DNA fragments 3456 bp and 924 bp in size and a 7273 bp *Eco*RV fragment (Figure 4.9). These fragment sizes are consistent with insertion (in the reverse orientation) of the 1136 bp *erm* gene into pCT0018. Probe DNA also hybridised to DNA fragments of the expected size for all positive controls; two *Dra*I (1014 bp and 3347 bp) and an *Eco*RV fragment (7273 bp) of strain DSE201 DNA, two *Dra*I (*ca*. 924 bp and 2765 bp) and an *Eco*RV fragment (9039 bp) from strain pKS951 co-integrate and plasmid pKS951 DNA, and a 1136 bp *Bam*HI fragment from plasmid pCT800. Probe DNA did not hybridise with the negative control DRDC8Sm* DNA.

Similarly, Southern hybridisation analysis of *Dra*I and *Eco*RV digested DNA from strain DSE952 showed that probe DNA hybridised to two *Dra*I DNA fragments (3291 bp and 1089 bp) and an *Eco*RV fragment (7273 bp) (Figure 4.10). This evidence was indicative of insertion (in the opposite orientation) of the 1136 bp *erm* gene cartridge into pCT0019. Data presented in Figure 4.10 also showed that probe DNA hybridised to DNA

fragments of the expected size for all positive controls; two *Dra*I (1014 bp and 3347) and an *Eco*RV fragment (7273 bp) of strain DSE201, two *Dra*I (*ca*. 1089 bp and 2599 bp) and an *Eco*RV fragment (*ca*. 9039 bp) from strain pKS952 co-integrate and plasmid pKS952 DNA, and a 1136 bp *Bam*HI fragment from plasmid pCT800. Probe DNA did not hybridise with the negative control DRDC8Sm* DNA.

Collectively, the data presented in Figure 4.8, Figure 4.9 and Figure 4.10 provided evidence to show that *L. monocytogenes* strains DSE951 and DSE952 are pCT0018::*erm* and pCT0019::*erm* insertion mutants, respectively.

4.3.3.3 Characterisation of *cutR*::*erm* strain DSE955

To provide evidence to show that strain DSE955 is a *cutR*::*erm* mutant, PCR analysis was conducted using the CuMutR/ermF2, CuTrM2R/ermF2, CuTrF/ermR2, CuTrM2F/ermR2, and CuTrM2F/CuTrM2R oligonucleotide pair combinations (refer to Table 2.7 for oligonucleotide description). These combinations were used based on the orientation of *erm* within *cutR* (as previously determined in Section 4.3.1). Oligonucleotides CuTrM2F and CuTrM2R were designed specifically to flank the DNA 5' and 3', respectively, of the allelic replacement mutation. The data presented in Figure 4.11 showed PCR amplicons indicative of insertion of the 1136 bp *erm* gene into *cutR*. Amplicons of the expected size were produced for the CuMutR/ermF2 (916 bp), CuTrM2R/ermF2 (1502 bp), CuTrF/ermR2 (1108 bp), CuTrM2F/ermR2 (1155 bp), and CuTrM2F/CuTrM2R (3019 bp) oligonucleotide pairs. The 1136 bp difference in amplicon size for DSE955 (3019 bp) and the positive control strain DRDC8Sm* (1883 bp) obtained when the CuTrM2F/CuTrM2R primer pair was used, is consistent with insertion of the *erm* gene into *cutR*. This was further confirmed by sequence analysis of the 3019 bp PCR product (refer to Appendix Q, page 346).

Southern hybridisation analysis of DNA isolated from strain DSE955 was used to confirm that the strain carries the *cutR*::*erm* insertion mutation. Probe DNA hybridised to two *Dra*I DNA fragments (1266 bp and 1085 bp) and an *Eco*RV fragment (7134 bp) of the predicted size (Figure 4.12). The size of these fragments is consistent with insertion of the 1136 bp *erm* gene cartridge into *cutR*. Probe DNA also hybridised to DNA fragments of the expected size for all positive controls; two *Dra*I fragments (1014 bp and 3347 bp) and

an *Eco*RV fragment (7273 bp) from strain DSE201, two *Dra*I fragments (*ca*. 1266 bp and 1862 bp) and an *Eco*RV fragment (*ca*. 8866 bp) from strain pKS955 co-integrate and plasmid pKS955 DNA, and a 1136 bp *Bam*HI fragment from plasmid pCT800. As expected, probe DNA did not hybridise with the negative control DRDC8Sm* DNA.

Collectively, the data presented in Figure 4.11 and Figure 4.12 provided substantial evidence to show that *L. monocytogenes* strain DSE955 is a *cutR*::*erm* insertion mutant.

4.3.4 Isolation of Plasmid-cured Variants of DRDC8

The *L. monocytogenes* strain DRDC8 derived mutant strains DSE201 (*ctpA*::*erm*) and DSE955 (*cutR*::*erm*), were cured of plasmid DNA by growth in the presence of acridine orange (refer to Section 2.18). Strain DSE201 is an isogenic derivative of strain DRDC8 that carries a *ctpA*::*erm* insertion mutation on plasmid pCT100. DSE201 variants cured of plasmid were identified by loss of erythromycin resistance following acridine orange treatment. DSE201 was serially cultured in BHI containing sub-inhibitory concentrations (10 μg mL^{-1}) of acridine orange. Single colonies were replica patched onto BHI agar supplemented with acridine orange (10 μg mL^{-1}) and BHI agar supplemented with Erm (8 μg mL^{-1}). A single Em^S, acridine orange resistant colony (strain DSE201PL) was selected and cultured for further analysis. Loss of plasmid DNA was confirmed by PCR analysis of DNA extracted from strain DSE201PL. PCR amplification of the *L. monocytogenes* chromosomal genes *hly* (p234/p319 oligonucleotide pair) and *cutR* (CuTrR/CuTrF oligonucleotide pair), but absence of amplification of plasmid marker DNA, *ctpA* (FB001/LM2004 oligonucleotide pair) and pCT0016 (FB1864/S12210R oligonucleotide pair) indicated that strain DSE201PL has been cured of plasmid pCT100 (Figure 4.13 Panel A).

A plasmid cured variant of the *cutR*::*erm* strain DSE955 was prepared as follows. As DSE955 lacks a selectable antibiotic resistance plasmid marker that could be used to identify plasmid cured variants of this strain, preliminary experiments were used to determine whether loss of the cadmium transport system encoded by pCT100 was associated with an increase in sensitivity to cadmium ions. To test this concept, the tolerance of strain DSE201PL to $CdSO_4$ was compared to the parental strain DSE201. Minimal inhibitory concentration (MIC) experiments (refer to Section 2.19) were used to

show that loss of plasmid DNA for strain DSE201PL is associated with a reduction in the MIC for $CdSO_4$. The MIC values of $CdSO_4$ for the plasmid cured strain DSE201PL and the parent strain DSE201 were 0.10 – 0.15 mM and 0.55 – 0.70 mM, respectively. Further testing showed that the control strain DSE201, but not the plasmid cured variant DSE201PL, was able to grow on BHI agar supplemented with 0.2 mM $CdSO_4$.

Loss of cadmium resistance was used to isolate DRDC8 *cutR*::*erm* mutants cured of plasmid pCT100. Acridine orange treated BHI cultures of DSE955 were replica plated on BHI agar supplemented with acridine orange (10 μg mL^{-1}) containing Em and on BHI agar supplemented with 0.2 mM $CdSO_4$. A single erythromycin resistant, cadmium sensitive (no growth on media supplemented with 0.2 mM $CdSO_4$) colony (DSE955PL) was selected and cultured for further analysis. This strain was confirmed as a *L. monocytogenes* derivative by PCR amplification of the chromosomal marker genes *hly* (p234/p319 oligonucleotide pair) and *cutR* (CuTrR/CuTrF oligonucleotide pair) (Figure 4.13 Panel B). PCR amplicons for plasmid markers, *ctpA* (LM2004/p1037 oligonucleotide pair) and pCT0016 (FB1864/S12210R oligonucleotide pair), could not be obtained. Together this data confirmed DSE955PL was a plasmid cured derivative of DRDC8 (Figure 4.13 Panel B).

4.3.5 Response of *L. monocytogenes* strains to Cation Stress.

4.3.5.1 MIC Assays

To analyse the tolerance of *L. monocytogenes* strains to copper and cadmium and to copper starvation, the minimal inhibitory concentration (MIC) of $CuSO_4$, $CdSO_4$ and 8-hydroxyquinoline[24] was determined for strains DSE955 (*cutR*::*erm*), DSE951 (pCT0018::*erm*) and DSE952 (pCT0019::*erm*), and plasmid-cured strains DSE201PL and DSE955PL (refer to Section 2.19). The parental strains DRDC8 and DSE201 (*ctpA*::*erm*) and other wild type *L. monocytogenes* isolates were used as control cultures. Cultures were grown on BHI agar supplemented $CuSO_4$, $CdSO_4$ and 8-hydroxyquinoline with incubation at 37ºC for 48 h.

[24] The chelating agent, 8-hydroxyquinoline, was used to deplete the BHI growth medium of free copper ions and create a copper starvation environment.

The MIC values for $CuSO_4$ for all *L. monocytogenes* strains tested are shown in Figure 4.14. The MIC values for mutant strains DSE201 (*ctpA*::*erm*), DSE951 (pCT0018::*erm*) and DSE952 (pCT0019::*erm*), the plasmid-cured strains DSE201PL and DSE955PL (*ca*. 16.8 – 17 mM) were significantly different ($P < 0.05$) to the MIC obtained for the wild type parental strain DRDC8 (*ca.* 20 mM). In addition, the MIC values for wild type strains KE795 and KE1003 were also significantly different from DRDC8 (*ca*. 17 – 18 mM) ($P < 0.05$). However, the MIC value for the *cutR*::*erm* mutant strain DSE955 was not significantly different from DRDC8 ($P = 0.1395$). Interestingly, the MIC of strain DSE955PL, a plasmid-cured variant of *cutR*::*erm* mutant strain DSE955, (*ca*. 4.3 mM), and strain EGD Kaufmann (*ca*. 10.7 mM) were significantly less than all other strains analysed.

The MIC values for 8-hydroxyquinoline for all *L. monocytogenes* strains tested are presented in Figure 4.15. The wild type strains KE795 and KE1003 exhibited greater tolerance to this chelating agent (MIC range 60 – 72 μM) than other strains analysed. Strains DRDC8 and EGD Kaufman tolerated levels to *ca*. 28 - 30 μM, while the mutant strains (DSE201 (*ctpA*::*erm*), DSE951 (pCT0018::*erm*), DSE952 (pCT0019::*erm*) and DSE955 (*cutR*::*erm*)) and plasmid cured strains (DSE201PL and DSE955PL) tolerated levels ranging between 13 – 17 μM. Importantly, the MIC values of 8-hydroxyquinoline for mutant strains DSE201, DSE951, DSE952 and DSE955 and plasmid-cured strains DSE201PL and DSE955PL were significantly different ($P < 0.05$) from the wild type parental strain DRDC8.

The MIC values for $CdSO_4$ for all *L. monocytogenes* strains tested are presented in Figure 4.16. The wild type strain EGD Kauffman, and mutant strains DSE201 (*ctpA*::*erm*) and DSE952 (pCT0019::*erm*) exhibited similar tolerance to $CdSO_4$ to that of DRDC8 (MIC range 0.50 – 0.70 μM) ($P > 0.05$). However, the MIC values for wild type strains KE1003 and KE795 and mutant strains DSE951 (pCT0018::*erm*) and DSE955 (*cutR*::*erm*) were significantly different ($P < 0.05$) from that of DRDC8 (MIC range 0.36 – 0.46 μM). Interestingly, the MIC value for plasmid-cured strains DSE201PL and DSE955PL were significantly lower than all other strains analysed. Growth of these strains was inhibited at values < 0.1 μM $CdSO_4$.

4.3.5.2 Growth Experiments

To determine the impact of subtoxic concentrations of $CuSO_4$ on the growth of *L. monocytogenes,* strains were cultured at 37°C in BHI broth with and without added 14 mM $CuSO_4$ (refer to methods described in Section 2.20). The culture absorbance (OD_{600}) for each strain was recorded over a 24 h period. The growth of mutant (DSE201 (*ctpA*::*erm*), DSE951 (pCT0018::*erm*), DSE952 (pCT0019::*erm*) and DSE955 (*cutR*::*erm*)) and plasmid cured strains (DSE201PL, DSE955PL) was compared with the parental strain (DRDC8) and other wild type *L. monocytogenes* isolates (EGD Kaufmann, KE795 and KE1003).

All strains cultured in BHI grew at approximately the same rate (Figure 4.17 Panel A), but grew at different rates when cultured in BHI with 14 mM $CuSO_4$ (Figure 4.17 Panel B). As expected from the MIC data for $CuSO_4$ (see Figure 4.14), growth of strains EGD Kaufmann and DSE955PL was impaired in the presence of 14 mM $CuSO_4$. By contrast, strain DRDC8 attained a culture absorbance of *ca*. 1.0 within 12 h incubation. Strains KE795 and KE1003 grew as rapidly as DRDC8 over the first 4 h of culture, but achieved a maximum culture absorbance of only 0.4 and 0.25 respectively. By 24 h the absorbance of KE795 and KE1003 was *ca*. 0.2 and 0.17, respectively. Conversely, mutant strains DSE201 (*ctpA*::*erm*), DSE955 (*cutR*::*erm*) and DSE952 (pCT0019::*erm*) did not grow appreciably for at least 4 h post inoculation of BHI with added $CuSO_4$. While the growth characteristics of DSE952 were similar to that of DSE955 for the first 12 h of culture, by 24 h the absorbance of DSE955 was equivalent to that of DRDC8, whereas the absorbance of DSE952 was *ca*. 0.57. By 24 h, the absorbance of DSE201 was also significantly less than that of DRDC8 (*ca*. 0.36). In addition, mutant strain DSE951 (pCT0018::*erm*) did not grow appreciably for at least 7 h post inoculation, but achieved a maximum culture absorbance equivalent to that of DSE952. The plasmid cured strain DSE201PL also impaired growth in BHI containing 14 mM $CuSO_4$, but achieved a maximum culture absorbance comparable to strain DSE201 by 24 h.

4.4 Discussion

The purpose of the work described in this chapter was to gather evidence to support the hypothesis that ORFs *cutR*, pCT0017, pCT0018 and pCT0019 are involved in copper

homeostasis. This was achieved by analysis of the impact of insertion mutations in these ORFs on the ability of *L. monocytogenes* strain DRDC8 to tolerate copper ion stress. In addition, the work described represents an evaluation of the role of plasmid associated genes carried by DRDC8 in cation (copper and cadmium) transport through analysis of the impact of loss of plasmid on cation tolerance. To investigate the potential interaction between the chromosomally-encoded ORF *cutR* and the plasmid-encoded genes, copper tolerance of a *cutR*::*erm* derivative of DRDC8 cured of plasmid pCT100 was compared to the wild type parent.

L. monocytogenes strain DRDC8 carrying insertion mutations within ORFs *cutR* (strain DSE955), pCT0018 (strain DSE951) and pCT0019 (strain DSE952) were constructed using the methods of allelic exchange. The principle of allelic exchange has been routinely used in studies of *L. monocytogenes*. The suicide shuttle vector pKSV7 was developed specifically to engineer allelic replacement of wild type alleles in Gram-positive bacteria such as *L. monocytogenes* (Smith & Youngman, 1992). The temperature permissive replicon of pKSV7 facilitated selection of integration of the pKSV7 based vectors containing insertion mutations into *L. monocytogenes* DNA, followed by integration of mutant alleles and excision of the vector via growth at a non-permissive temperature. *L. monocytogenes* strains in which wild type ORFs were replaced by the mutated allele were detected by antibiotic selection and confirmed by PCR and Southern hybridisation analysis.

Each of the mutants were created by insertion of a 1136 bp *Bam*HI *ermR* gene cassette derived from plasmid pGI21 that was originally sourced from pAMβ1 (Clewell, 1981). Although this cassette was not designed specifically to create non-polar transcriptional insertion mutants, the nucleotide sequence encoding the *ermR* gene (refer to Appendix J, page 335) does not include sequence characteristic of a rho-independent terminator. Nevertheless, there is a possibility that insertion of this cassette within a gene may create polar mutations that could potentially impact on expression of other cotranscribed genes. The impact of polar *vs* non-polar insertion mutations will be discussed.

Despite repeated attempts, a DRDC8 strain carrying an insertion mutation in ORF pCT0017 could not be created without significant rearrangement of 5' flanking DNA. PCR and Southern hybridisation analysis of 26 putative *L. monocytogenes* pCT0017::*erm*

mutants indicated that these constructs were likely to be the result of partial resolution of a pKS950 cointegrate. While pCT0017::*erm* was successfully exchanged from plasmid pKS950 to DRDC8 DNA, 5' flanking DNA was either excised or rearranged in all of the strains analysed. PCR analysis confirmed that 3' flanking DNA was not affected and remained intact. Consequently it was concluded that it may not be possible to create a defined pCT0017::*erm* mutant using this method. The underlying mechanism by which these rearrangements occurred is not known, however, they are unlikely to involve vector DNA as the absence of the *cat* selection marker in all 26 strain analysed indicated that vector DNA had been excised. In view of the identified rearrangements and the possible effects on expression of flanking genes, none of these mutants were used in subsequent studies of cation stress. Future studies should aim to resolve this issue by creating deletion mutations or by the use of conditional mutations.

It is interesting to speculate that creation of a pCT0017::*erm* mutation in strain DRDC8 may not be possible. If pCT0017 encodes a CopY-type negative transcriptional regulator that is part of a *cop*-like operon (comprising pCT0017, pCT0018, pCT0019 and *ctpA*), a non-polar insertion mutation within pCT0017, may significantly affect the pattern of expression of pCT0018, pCT0019 and also *ctpA*. Certainly, in *E. hirae,* disruption of *copY* lead to unregulated overexpression of the CopA and CopB copper transporters, hyper-resistance to copper and also reduced growth rates (copper deficiency) under conditions of limiting copper (Odermatt & Solioz, 1995). Unlike *E. hirae*, a *copB* homolog has not been identified in DRDC8. As CtpA is thought to be involved in Cu^{2+} uptake (Francis & Thomas, 1997a), a pCT0017 mutation may lead to excess free copper ions in the cytoplasm in a system that is not complemented by an over-expressed CopB equivalent. High concentrations of free copper ions within the cytoplasm would be autocatalytic for generation of toxic hydroxyl radicals that in turn, would lead to cell death. If these defects were lethal to cells, it is not surprising that following selection for allelic replacement mutants, surviving cells contained permissive genetic rearrangements that abrogated the effect of the expected allelic replacement mutation in ORF pCT10017.

Conversely, if the *erm* insertion in ORF pCT0017 resulted in a polar mutation, expression of pCT0017 and any cotranscribed genes would be affected. Assuming the mutation only affects genes that comprise the proposed *cop* operon (pCT0017, pCT0018,

pCT0019 and *ctpA*) in DRDC8, a polar mutation would be expected to result in a phenotype consistent with strains cured of the large plasmid ie. DSE201PL. However, it is unclear why polar mutation would lead to selection of strains carrying the described genetic rearrangements for putative pCT0017 mutants.

In addition to the creation of specific allelic replacement mutants (strains DSE951 (pCT0018::*erm*), DSE952 (pCT0019::*erm*) and DSE955 (*cutR*::*erm*)), mutant strains DSE201 (*ctpA*::*erm*) and DSE955 were cured of plasmid DNA to create strains DSE201PL and DSE955PL, respectively. To evaluate the impact of these mutations and loss of plasmid DNA on tolerance to copper, MIC and growth experiments were conducted. These experiments aimed to provide phenotypic evidence to demonstrate roles for ORFs *cutR*, pCT0018 and pCT0019 and plasmid DNA in copper ion tolerance for *L. monocytogenes*. The MIC for $CuSO_4$ for the pCT0018, pCT0019 and *ctpA* mutant strains were similar, but significantly different from that of the wild type DRDC8 strain. Concomitant changes in the growth profile of cultures of these mutants were also observed in the presence of 14 mM $CuSO_4$, for which the growth potential was significantly reduced compared to DRDC8. In addition, DRDC8 cured of the large plasmid (strain DSE201PL) exhibited an MIC value and growth profile similar to these insertion mutants. Interestingly, although cultures of the *cutR* mutant strain DSE955 grew more slowly than DRDC8 in the presence of 14 mM $CuSO_4$, it ultimately achieved a similar growth potential to the DRDC8 wild type strain by 24 h of incubation. These results are consistent with the fact that the MIC for $CuSO_4$ for this *cutR* mutant strain was not significantly different from that of DRDC8. This result suggested that an alternative copper homeostasis mechanism, such as that encoded by plasmid pCT100, compensated for the loss of *cutR* and enabled the bacterium to overcome toxic conditions imposed by high levels of environmental copper ions.

Taken together, this data indicated that pCT0018, pCT0019, *ctpA* and *cutR* are implicated in copper tolerance. Inactivation of any of these genes, or removal of the plasmid-encoded genes by curing DRDC8 of plasmid DNA, had a significant effect on tolerance and growth potential. These results are comparable to those published by Odermatt *et al*., (1993), where the marked sensitivity of strains DSE951, DSE952, DSE201 and DSE201PL is similar to the copper sensitive response observed for *E. hirae copB*

mutants. It therefore tempting to conclude that the DSE955 (*cutR*) mutant displays a response to copper indicative of copper dependence as shown by *E. hirae copA* mutants. Based on conclusions by Odermatt *et al.*, (1993) this suggested that *ctpA* may function as a copper efflux transporter, while *cutR* may function as an copper influx transporter. This conclusion is contrary with that published by Francis and Thomas, (1997a). However, that study was limited to *ctpA* mutants and lack of definitive DNA sequence that might have provided insights into the genetic organisation and function of other *cop* genes in *L. monocytogenes* DRDC8.

Furthermore, the results obtained showed that the combination of a *cutR* mutation and loss of plasmid pCT100 rendered cells completely incapable of growth in the presence of high levels (14 mM $CuSO_4$) of copper. Collectively, these observations suggest that expression of *cutR* and plasmid associated genes (ie. pCT0017, pCT0018, pCT0019 and *ctpA*) are critical for tolerance of *L. monocytogenes* to high concentrations of copper ions. As plasmid pCT100 carries at least nine ORFs that potentially encode proteins involved copper ion tolerance, including a putative multicopper oxidase (pCT0025, refer to Chapter 3), it is not surprising that loss of plasmid DNA was associated with increased sensitivity to copper. Certainly, it has been shown in *E. coli* that mutation of the *cueO* gene which encodes a 516 amino acid multicopper oxidase (CueO), results in copper sensitivity (Grass & Rensing, 2001a). Similarly, it is not surprising that the disruption of the putative copper-translocating P-type ATPase encoded by *cutR*, combined with loss of plasmid DNA, renders cells incapable of growth in conditions of copper excess, where all available mechanisms to maintain copper ions homeostasis may have been eliminated.

Significantly, wild type *L. monocytogenes* strains KE795, KE1003 and EGD Kaufmann exhibited tolerance for copper significantly less than that of strain DRDC8. Strains KE795 and KE1003, which do not carry *ctpA*, had MIC values and growth profiles similar to that of the DRDC8 insertion mutants and the plasmid cured strain (DSE201PL). However, wild type strain EGD Kaufmann, which does not carry any ORFs associated with the DRDC8 putative copper gene cluster, displayed an intolerance to copper comparable to the *cutR*::*erm* plasmid cured strain DSE955PL. Strain EGD Kaufmann was completely incapable of growth in the presence of high levels (14 mM $CuSO_4$). These findings support the contention that the cluster of pCT100 encoded copper genes in DRDC8 are

important for copper tolerance. Nevertheless, strains KE795, KE1003 and EGD Kaufmann, are likely to utilise alternative mechanisms to DRDC8 to maintain copper homeostasis. Consequently, these strains may be less tolerant to copper than strain DRDC8 in the natural environment. It is interesting to speculate that acquisition of pCT100 or the putative copper gene cluster by these strains, particularly the copper sensitive strain EGD Kaufmann, may result in increased tolerance to copper.

Although the results presented directly implicate pCT0019, pCT0018, *ctpA* and *cutR* in copper tolerance, the role of other plasmid associated genes in tolerance cannot be excluded. It is also unknown whether other chromosomal genes are influenced by this combination of disruptions/deletions. Separate experiments that use defined DRDC8 strains containing *cutR* mutation together with deletions of the pCT0017, pCT0018, pCT0019 and *ctpA* genes (either individually or combinations thereof) need to be performed to definitively link these genes in copper tolerance. Ideally this could first be achieved by cloning pCT0017, pCT0018, pCT0019 and *ctpA* into a non DRDC8 background such as *L. monocytogenes* strain EGD Kaufmann. This strain carries the *cutR* gene and is sensitive to low concentrations of copper. The advantage of this approach is that the function of the *cop* genes encoded on the DRDC8 plasmid can be examined in the absence of other plasmid genes. If acquisition of the DRDC8 plasmid-encoded genes resulted in increased tolerance to copper to levels tolerated by DRDC8, then this would provide strong evidence for the role of these genes in tolerance. Further work could confirm this result by examining the effects of single and double deletions of individual genes on tolerance.

While it is clear that ORFs pCT0018, pCT0019, *ctpA* and *cutR*, and probably other plasmid-encoded genes have an important role to play in the growth of *L. monocytogenes* in high copper environments, the normal nutritional requirement of this bacterium in low copper environments may also be influenced by these genes and their gene products. Copper starvation conditions can be induced in laboratory media by addition of chemicals that sequester this cation eg. 8-hydroxyquinoline. This agent has a high binding coefficient for copper ions compared to other divalent cations (Dawson *et al.*, 1986). 8-hydroxyquinoline has been used to functionally characterise the CopA and CopB copper transport system of *E. hirae* (Odermatt *et al.*, 1993; Odermatt *et al.*, 1994). *E. hirae copA*$^-$

mutants were unable to grow in Cu^{2+} limiting medium induced by 8-hydroxyquinoline, thus suggesting that CopA is necessary for Cu^{2+} influx in *E. hirae*. Likewise, Francis and Thomas, (1997a) also deployed this agent to evaluate the effects of *ctpA* mutants grown under copper starvation conditions. This study concluded that growth of *ctpA* mutants in BHI broth containing 8-hydroxyquinoline was restricted in response to depletion of copper from the media; indicating that *ctpA* was involved in copper ion transport in *L. monocytogenes*.

In the present study, none of the *L. monocytogenes* mutants or the plasmid cured strains tested were able to grow at 8-hydroxyquinoline concentrations that were limiting for strain DRDC8. Indeed, the recorded MIC values for these strains were approximately half that of DRDC8. This implied that the mutants and plasmid cured strains have a reduced capability to obtain the concentration of copper ions necessary for growth compared to wild type DRDC8. Hii, (2009) however, presented data to show that 5 μM 8-hydroxyquinoline had no effect on growth of these mutants and plasmid cured strains during growth in *Listeria* enrichment broth. Based on results presented in the present study, this contrasting result is likely to be due to the fact that concentrations of the chelating agent used by Hii, (2009) were insufficient to sequester copper within the growth media used in that study. In view of the effect of 8-hydroxyquinoline on growth of the strains tested, it is likely that *cutR* and the plasmid-encoded ORFs pCT0018, pCT0019 and *ctpA* are involved in transport of copper. Loss of these genes did impact on the ability of *L. monocytogenes* to acquire dietary copper requirements.

Although it was not confirmed by analytical methods, it is likely that the addition of 8-hydroxyquinoline to the culture medium leads to a depletion of the essential trace element, copper. However, it is also possible the effect of this chelating agent on bacterial growth, particularly at high concentrations, may reflect (at least in part) a toxic response. Indeed, 8-hydroxyquinoline is a well-known fungicide (Rigler & Greathouse, 1941) and bactericide (Albert *et al.*, 1947) manufactured by companies for use in agricultural systems and industry. Formation of copper 8-hydroxyquinoline complexes could create a toxic agent to which some strains of bacteria are more susceptible than others. However, it unknown whether 8-hydroxyquinoline reduces copper induced oxidative stress more for some strains of bacteria than for others.

Furthermore, it is possible that 8-hydroxyquinoline is not a copper-specific chelator. The recorded MICs for this chelating agent may also be the result of depletion of other essential cations. However, the effectiveness of 8-hydroxyquinoline as a chelator of copper ions has been previously reported. Dawson *et al.*, (1986) claimed that this chelator possessed a comparatively high binding coefficient for copper ions, relative to other divalent cations. To address the issue of selectivity, it would be of interest for future studies to repeat these experiments using alternative chelating agents such as the copper specific chelators BCS (bathocuproine sulphonate) and TTM (tetrathiomolybdate), or other known copper chelators such as TEPA (tetraethylenepentamine) and DDC (diethyldithiocarbamic acid). Nevertheless, the results presented in this study are consistent with the growth limiting effects of 8-hydroxyquinoline for *E. hirae* $CopA^-$ mutants (Odermatt *et al.*, 1993; Odermatt *et al.*, 1994) and *L. monocytogenes ctpA* mutants (Francis and Thomas, 1997a). Whether this effect is directly related to sequestration of available copper has not been demonstrated. Notably, the wild type strains KE1003 and KE795 tolerated higher concentrations of 8-hydroxyquinoline compared to strain DRDC8. This observation may simply reflect strain to strain variation in tolerance for this chelating agent, rather than an enhanced ability to grow in copper depleted media.

Interestingly, MIC experiments conducted in the presence of $CdSO_4$ identified a potential linkage between copper and cadmium tolerance in *L. monocytogenes* strain DRDC8. Loss of plasmid DNA for strain DRDC8 was shown to be associated with a significant decrease in tolerance to cadmium ions, which is consistent with loss of ORFs (pCT0007 and pCT0008, refer to Section 3.3.6.4) that encode polypeptide sequences that are similar to proteins involved cadmium efflux. These experiments also showed that mutation in *cutR* (strain DSE955) is associated with a decreased tolerance to cadmium ions, although loss of both *cutR* and plasmid pCT100 (strain DSE955PL) decreased the cadmium tolerance to a level equal to that of a plasmid cured wild type strain (DSE201PL). Similarly, the MIC value for the pCT0018::*erm* strain DSE951 was significantly less than that of the parental strain DRDC8.

The existence of a gene involved in both copper homeostasis and cadmium resistance has been previously described. The *B. subtilis* chromosomal *copZ* gene encodes a protein that acts as a copper chaperone in copper homeostasis and also influences cadmium

resistance via regulation of *cadA* expression (Solovieva & Entian, 2004). This study demonstrated both copper and cadmium activation of the *copZA* operon. A *copA* deletion mutant was sensitive to copper, whereas a *copZ* deletion resulted in an increased sensitivity to both copper and cadmium. This is consistent with data gathered in the present study. Mutation of the *copA* equivalent gene *ctpA* (strain DSE201) did not affect cadmium sensitivity, however, *cutR* and pCT0018 mutations resulted in increased sensitivity. Taken together, this data suggested that for strain DRDC8, proteins encoded by *cutR* and pCT0018 that are implicated in copper tolerance, may also play a role in cadmium tolerance. The gene products of these ORFs may have metallochaperone like properties and act in the intracellular trafficking of metal ions (O'Halloran & Culotta, 2000). It is also possible that cadmium activates expression of copper homeostasis genes in DRDC8, however, further investigation is required to substantiate if an analogous association exists in strain DRDC8.

In summary, further research is required to gather a comprehensive understanding of the implication of these gene disruptions on gene expression and maintenance of copper homeostasis in strain DRDC8 and other wild type *L. monocytogenes* strains. Future studies should aim to create and functionally analyse a *ctpA*$^-$ and *cutR*$^-$ double deletion mutant. A comparative analysis of uptake and accumulation of radiolabelled copper ions in the cell of the double mutant and the *cutR*::*erm*, pCT0018::*erm* and pCT0019::*erm* mutants and plasmid-cured strains using atomic absorption spectroscopy would provide a more comprehensive understanding of the functionality of these genes. In addition, sections of *Listeria* cells grown in high concentration of copper could be analysed to identify where the copper is precipitated or accumulated. RT PCR analysis would also be useful in analysing gene expression under different copper ion concentrations.

4.5 Conclusions

The experimental data presented in this chapter has provided substantial evidence to show that ORFs *cutR*, pCT0018 and pCT0019 are involved in copper ion tolerance in *L. monocytogenes* strain DRDC8. The data gathered also showed that plasmid-encoded genes are required for tolerance of *L. monocytogenes* to both copper and cadmium stress. In addition, *cutR* and plasmid-encoded genes are critical for growth of

L. monocytogenes in the presence of high concentrations of copper. This suggested that both plasmid and chromosomal mechanisms are likely to be utilised to maintain in copper ion homeostasis in strain DRDC8. It is possible that *cutR* and ORF pCT0018 not only play a role in copper tolerance but also play associative roles in cadmium tolerance. It is also possible that regulation of expression of these genes is both copper and cadmium responsive. Interestingly, an *erm* insertion mutation in ORF pCT0017, which is predicted to encode a CopY-like copper-responsive transcriptional repressor protein, could not be created in *L. monocytogenes*. Mutation of this gene may result in loss of regulatory control of other genes involved in copper homeostasis and thus create an intracellular environment which is lethal for the bacterium. The function of the protein encoded by pCT0017 is investigated in Chapter 5 of this thesis.

Figure 4.1: PCR mutagenesis of ORFs pCT0017, pCT0018, pCT0019 and *cutR*.

*Bam*HI sites were introduced into in ORFs pCT0017 (A), pCT0018 (B), pCT0019 (C) and *cutR* (D) via nucleotide changes by overlap extension PCR mutagenesis. The location of oligonucleotides pairs MokFF/MokBR and MokBF/MokFR relative to pCT0017, FBdef/FBEBR and FBEBF/p1037 relative to pCT0018, FBdef/FBDBR and FBDBF/p1037 relative to pCT0019, and CuTrF/CuBamR and CuBamF/CuMutR relative to *cutR* are shown. These oligonucleotide pairs were designed to amplify overlapping DNA fragments of each ORF. The nucleotide sequence of oligonucleotides MokBR, MokBF, FBEBR, FBEBF, CuBamR and CuBamF were designed specifically to introduce a *Bam*HI site (GGATCC) into the respective ORF. The nucleotide length of each ORF and amplified PCR product is shown accordingly.

Diagrams not drawn to scale.

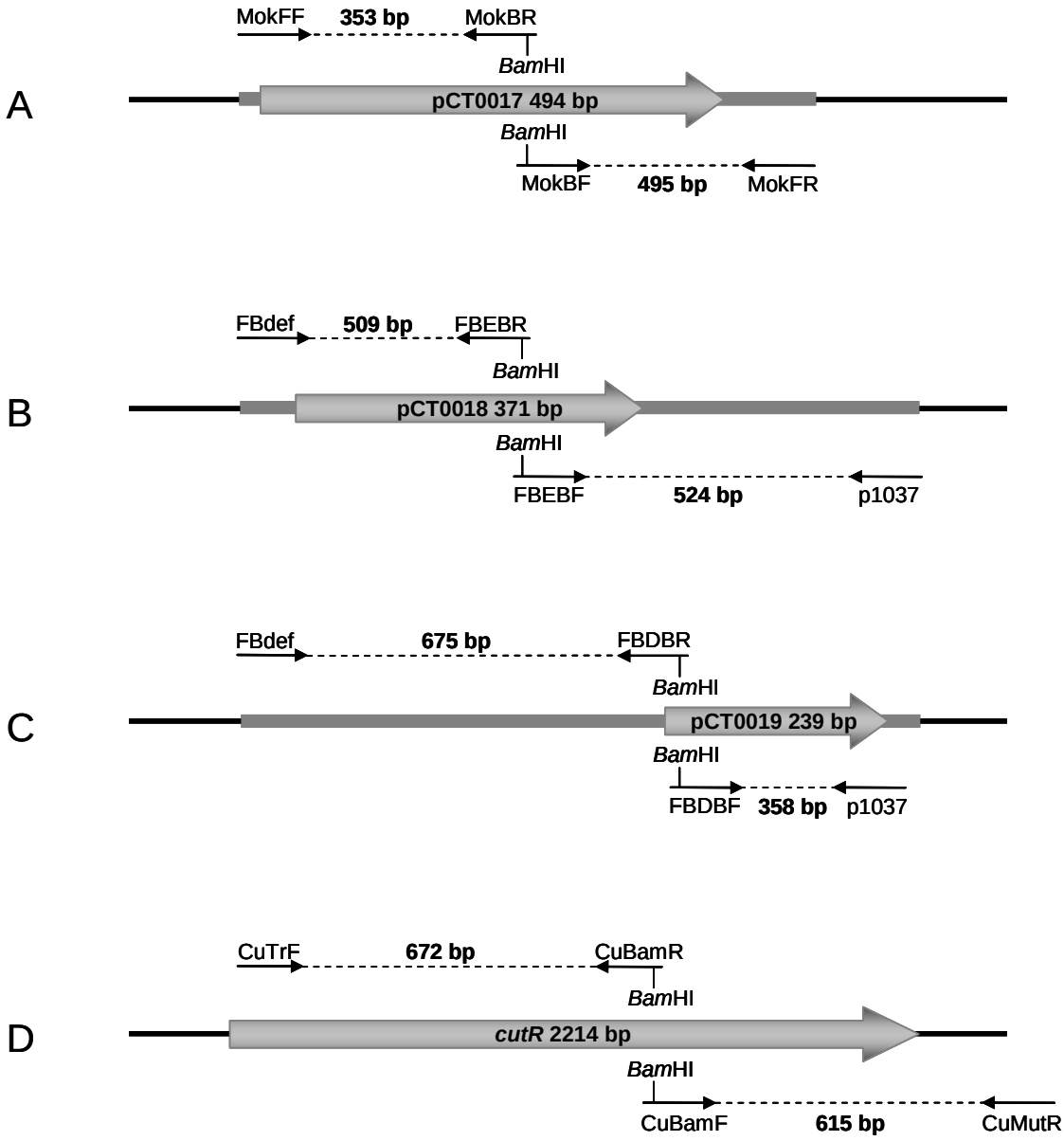
A
MokFF
353 bp
MokBR
BamHI
pCT0017 494 bp
BamHI
MokBF
495 bp
MokFR
B
FBdef
509 bp
FBEBR
BamHI
pCT0018 371 bp
BamHI
FBEBF
524 bp
p1037
C
FBdef
675 bp
FBDBR
BamHI
pCT0019 239 bp
BamHI
FBDBF
358 bp
p1037
D
CuTrF
672 bp
CuBamR
BamHI
cutR 2214 bp
BamHI
CuBamF
615 bp
CuMutR

Figure 4.2: Construction of *erm* insertion mutations.

PCR products generated using overlap extension PCR to introduce *Bam*HI sites into ORFs pCT0017, pCT0018, pCT0019 and *cutR* were ligated with pGEM®-T Easy cloning vector to create plasmids pCT750 (pCT0017), pCT751 (pCT0018), pCT752 (pCT0019) and pCT755 (*cutR*) (see Figure 4.3 for confirmation by restriction enzyme digestion). Plasmids pCT750, pCT751, pCT752 and pCT755 were digested with *Bam*HI and ligated with an erythromycin resistance cartridge (*erm*) carried on a *Bam*HI DNA fragment derived from plasmid pG121 to create plasmids pCT850 (pCT0017::*erm*), pCT851 (pCT0018::*erm*), pCT852 (pCT0019:*erm*) and pCT855 (*cutR*::*erm*). DNA fragments carrying pCT0017::*erm*, pCT0018::*erm*, pCT0019::*erm* and *cutR*::*erm* were isolated from plasmids pCT850, pCT851, pCT852 and pCT855 through *Eco*RI digestion.

Abbreviations: Amp^R, ampicillin resistance cartridge; f1 *ori*, pGEM®-T Easy origin of replication; *lacZ,* β-galactosidase gene; MCS, multiple cloning site.

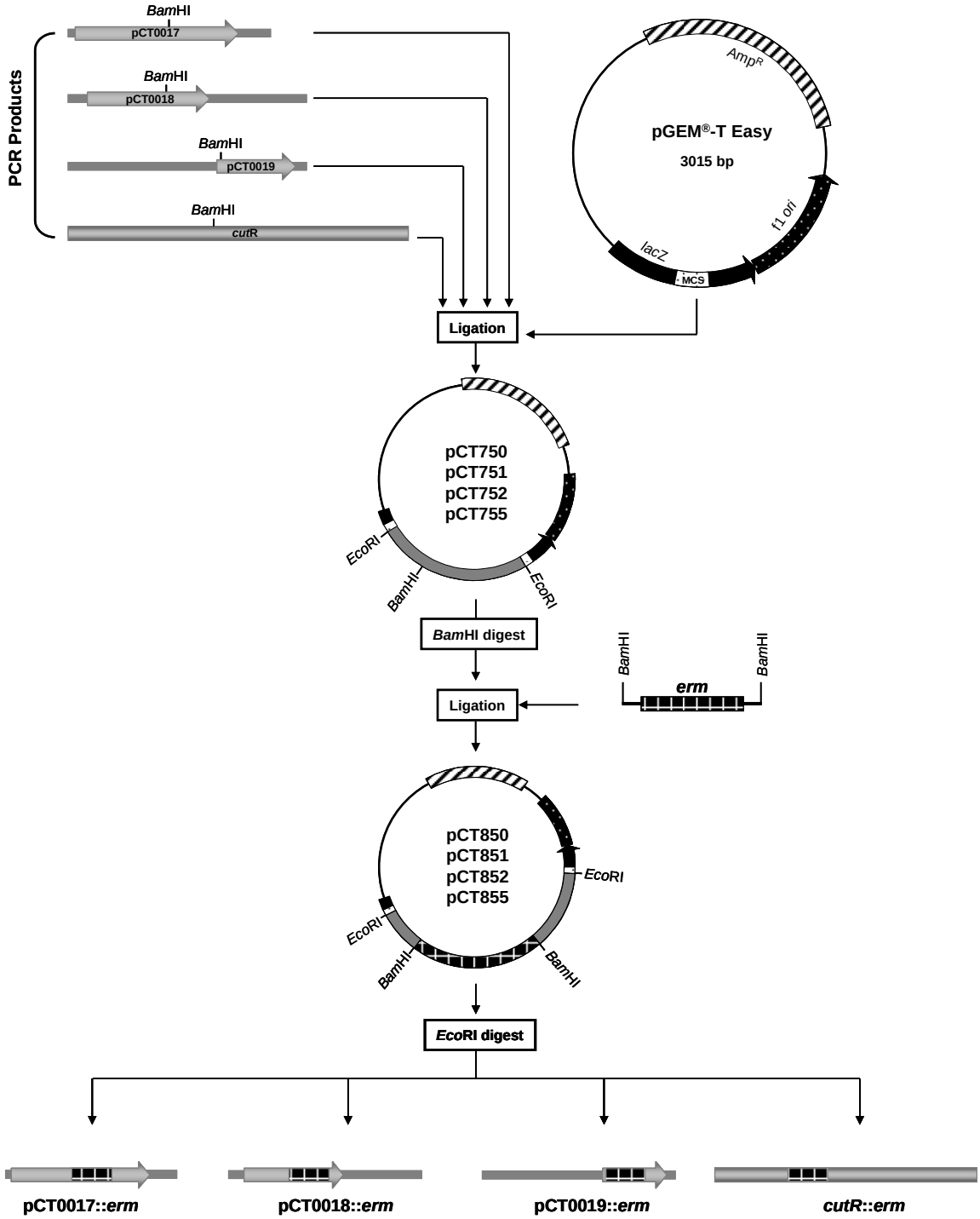
PCR Products
BamHI
pCT0017
BamHI
pCT0018
BamHI
pCT0019
BamHI
cutR
AmpR
pGEM®-T Easy
3015 bp
f1 ori
lacZ
MCS
Ligation
pCT750
pCT751
pCT752
pCT755
EcoRI
BamHI
EcoRI
BamHI digest
BamHI
erm
BamHI
Ligation
pCT850
pCT851
pCT852
pCT855
EcoRI
EcoRI
BamHI
BamHI
EcoRI digest
pCT0017::erm
pCT0018::erm
pCT0019::erm
cutR::erm

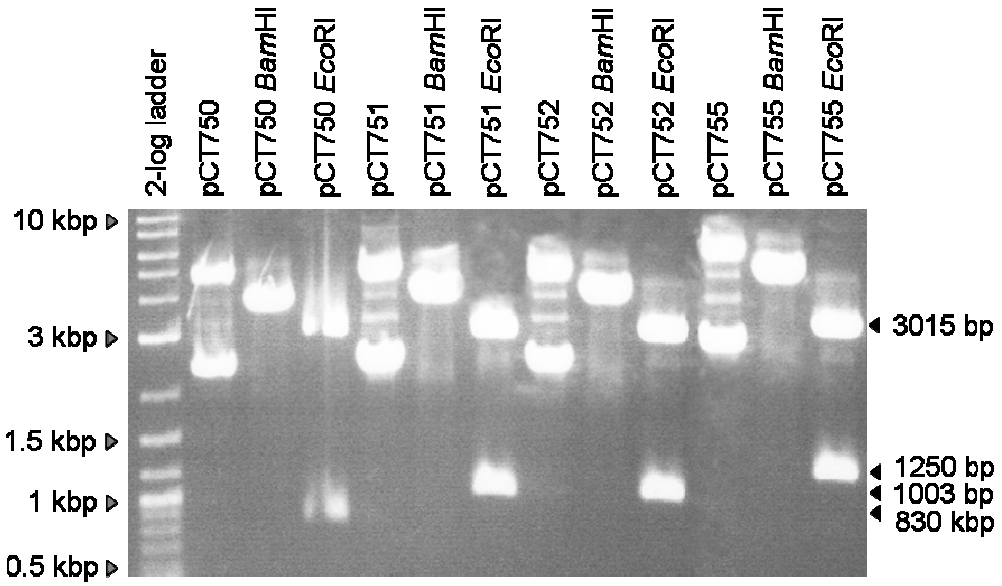

Figure 4.3: Restriction digestion of plasmids pCT750, pCT751, pCT752 and pCT755.

Plasmids pCT750, pCT751, pCT752 and pCT755 were constructed by cloning PCR products containing introduced *Bam*HI sites into ORFs pCT0017, pCT0018, pCT0019 and *cutR* into pGEM®-T Easy (refer to Figure 4.2). *Bam*HI digestion of plasmids pCT750, pCT751, pCT752 and pCT755 yielded a single DNA fragment of the expected size for all plasmids. *Eco*RI digestion yielded two DNA fragments of the expected size, one representing pGEM®-T Easy (3015 bp) and the other the respective inserted PCR product (830, 1003 or 1250 bp). Undigested samples of plasmids pCT750, pCT751, pCT752 and pCT755 were included.

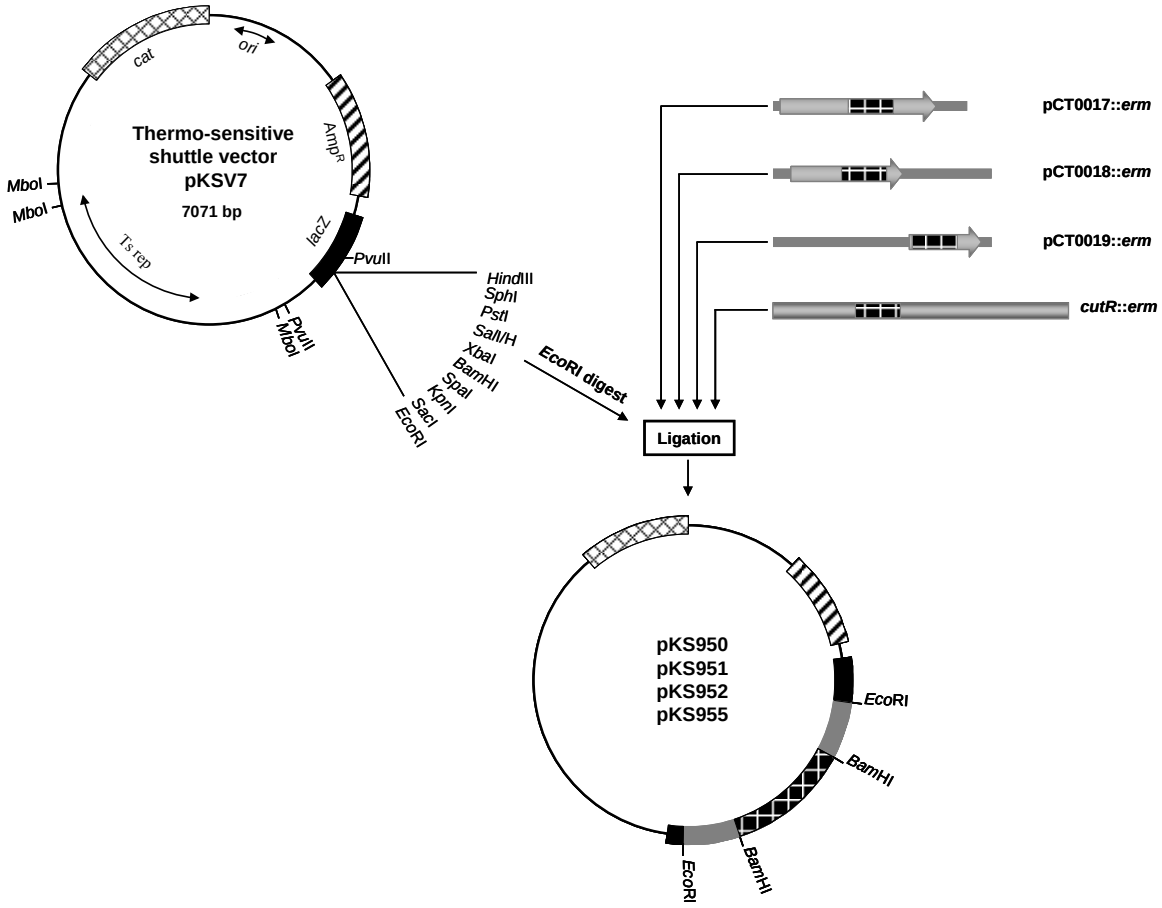

Figure 4.4: Construction of plasmids pKS950, pKS951, pKS952 and pKS955

*Eco*RI DNA fragments carrying *erm* insertion mutations in ORFs pCT0017, pCT0018, pCT0019 and *cutR* isolated from plasmids pCT850, pCT851, pCT852 and pCT855 (see Figure 4.2) were ligated with *Eco*RI digested plasmid pKSV7 to create plasmids pCT950 (carries pCT0017::*erm*), pCT951 (carries pCT0018::*erm*), pCT952 (carries pCT0019::*erm*) and pCT955 (carries *cutR*::*erm*).

Abbreviations: Amp^R, ampicillin resistance gene for selection in *E. coli*; *cat*, chloramphenicol resistance gene for selection in Gram-positive bacteria; Ts rep, temperature sensitive origin of replication; *lacZ,* β-galactosidase gene; *ori*, *E. coli* origin of replication.

Figure 4.5: PCR analysis of the putative pCT0017::*erm* mutant strain DSE950.

Panel A. Products **a** (1496 bp) and **b** (645 bp) were amplified by PCR from DNA extracted from strain DSE950 using the p2037/ermF2 and ermR/ermF oligonucleotide pairs, respectively. Amplicons were not produced using the FB1865/ermR2 or FB1865/p2037 oligonucleotide pairs. Amplicons were also not produced from the no DNA negative (-ve) controls for all of the primer pairs.

Panel B. Diagrammatic representation of the theoretical *erm* insertion in ORF pCT0017 in strain DSE950. The relative position of oligonucleotide pairs specifically designed to amplify corresponding DNA fragments (product **a** and **b**) within this region are shown. The respective nucleotide sequence for each oligonucleotide is listed in Table 2.7. Regions where DNA was not amplified by the corresponding oligonucleotide pair are denoted by the grey dashed line and X.

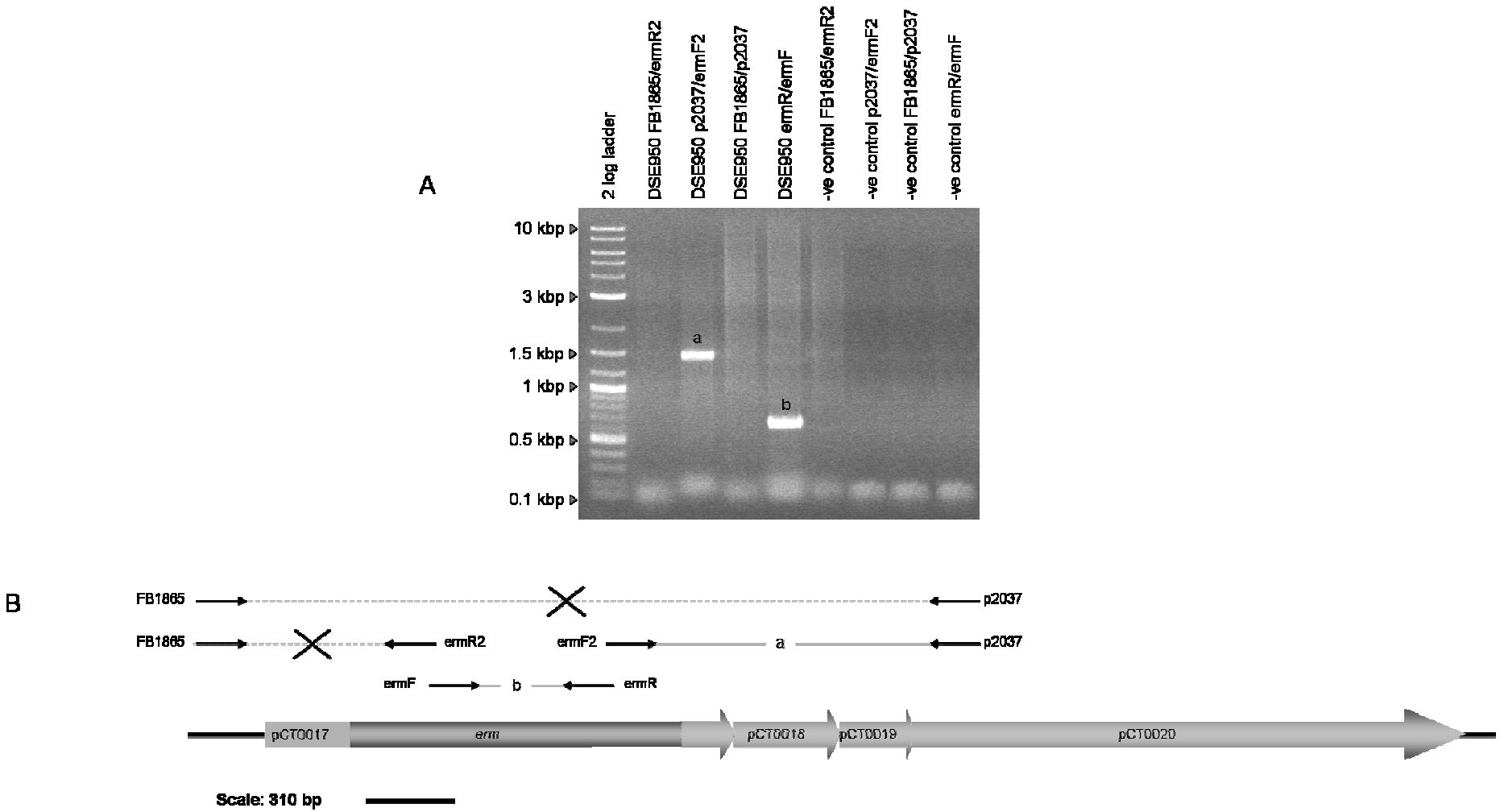
A
2 log ladder
DSE950 FB1865/ermR2
DSE950 p2037/ermF2
DSE950 FB1865/p2037
DSE950 ermR/ermF
-ve control FB1865/ermR2
-ve control p2037/ermF2
-ve control FB1865/p2037
-ve control ermR/ermF
10 kbp
3 kbp
1.5 kbp
1 kbp
0.5 kbp
0.1 kbp
a
b
B
FB1865
p2037
FB1865
ermR2
ermF2
a
p2037
ermF
b
ermR
pCT0017
erm
pCT0018
pCT0019
pCT0020
Scale: 310 bp

Figure 4.6: PCR analysis of strain DSE950.

Panel A. Product **a** (2219 bp) was amplified by PCR from DNA extracted from strain DSE950 using the MokFF/FB003 oligonucleotide pair. A PCR product 1083 bp in size was also amplified from the positive control strain DRDC8Sm* DNA using the same primer pair. No product was amplified from DSE950 DNA using the FB1863/S12210 oligonucleotide pair, however a 1427 bp product was amplified from DRDC8Sm* DNA using the same primer pair. Amplicons were not produced from the no DNA negative (-ve) controls for any primer pair.

Panel B. Diagrammatic representation of the theoretical *erm* insertion in ORF pCT0017 in strain DSE950. The relative position of oligonucleotide pairs specifically designed to amplify corresponding DNA fragments (product **a**) within this region are shown. The respective nucleotide sequence for each oligonucleotide is listed in Table 2.7. The region where DNA was not amplified by the FB1863/S12210 primer pair is denoted by the grey dashed line and X.

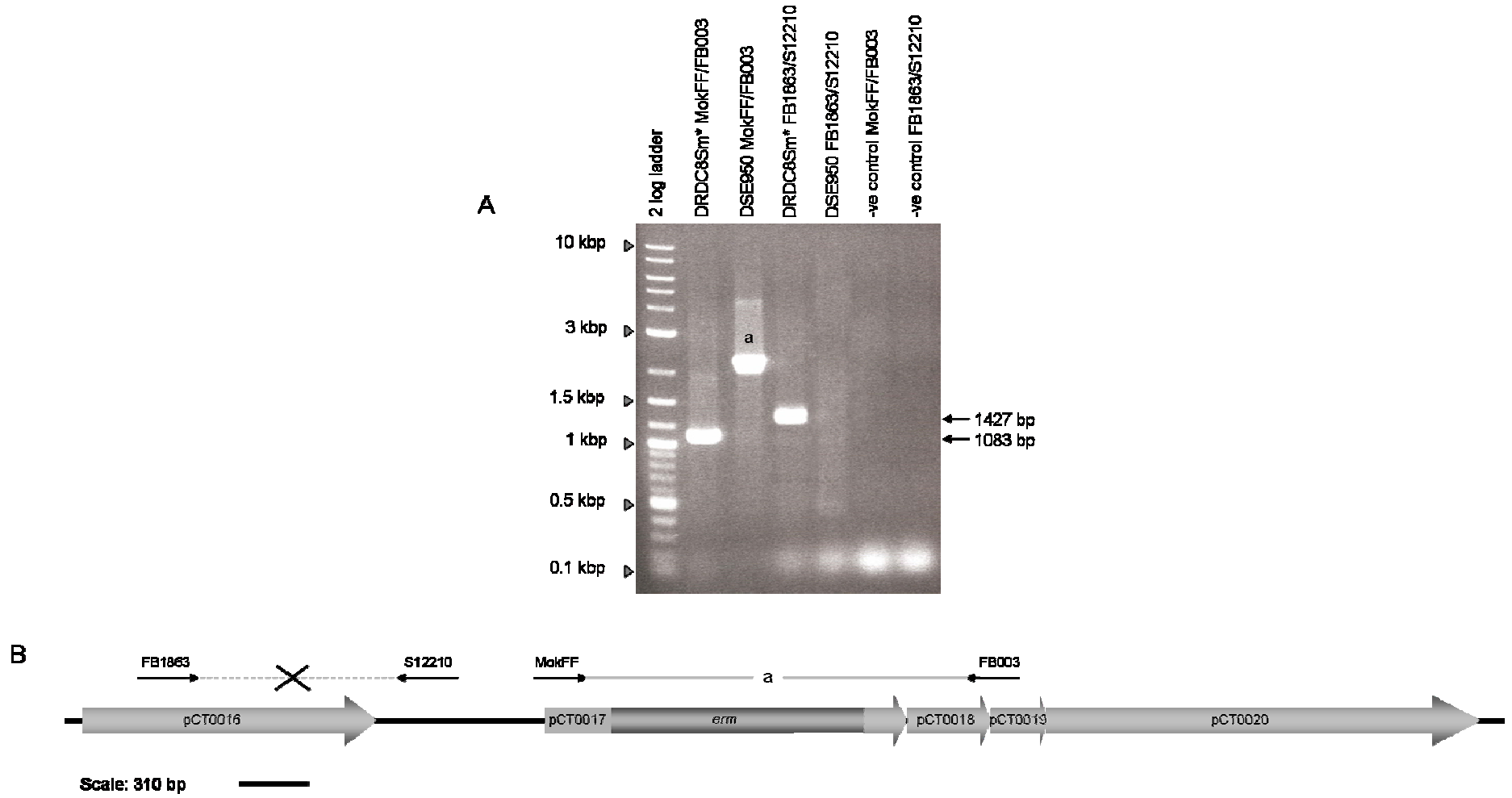
A
2 log ladder
DRDC8Sm* MokFF/FB003
DSE950 MokFF/FB003
DRDC8Sm* FB1863/S12210
DSE950 FB1863/S12210
-ve control MokFF/FB003
-ve control FB1863/S12210
10 kbp
3 kbp
1.5 kbp
1 kbp
0.5 kbp
0.1 kbp
a
1427 bp
1083 bp
B
FB1863
S12210
MokFF
a
FB003
pCT0016
pCT0017
erm
pCT0018
pCT0019
pCT0020
Scale: 310 bp

Figure 4.7: Southern hybridisation analysis of strain DSE950.

Panel A. *Dra*I digested DNA prepared from *L. monocytogenes* strain DSE950 was probed with a digoxigenin-labelled 645 bp *erm* fragment. Probe DNA hybridised to two DSE950 *Dra*I DNA fragments 1215 bp (**a**) and *ca*. 1718 in size. Labelled probe hybridised to *Dra*I DNA fragments from positive control strains DSE201 (1014 bp and 3347 bp) and pKS950 co-integrate (*ca*. 1215 bp and 1718 bp), and plasmid pKS950 (*ca*. 1215 bp and 1718 bp). Probe DNA also hybridised to the 1136 bp *Bam*HI *erm* fragment of plasmid pCT800. Labelled probe did not hybridise with DNA from the DRDC8Sm* negative control.

Panel B. *Eco*RV digested DSE950 DNA was probed with a digoxigenin-labelled 645 bp fragment of *erm*. Probe DNA hybridised to an *Eco*RV DSE950 DNA fragment *ca*. 6900 bp in size. Labelled probe hybridised to *Eco*RV DNA fragments for positive control strains DSE201 (7273 bp) and pKS950 co-integrate (*ca*. 8995 bp), and plasmid pKS950 (*ca*. 8995 bp). Probe DNA also hybridised to the 1136 bp *Bam*HI *erm* fragment of plasmid pCT800. Labelled probe did not hybridise with DNA from the DRDC8Sm* negative control.

Panel C. Diagrammatic representation of the theoretical *erm* insertion in ORF pCT0017 in strain DSE950. The relative position of all *Dra*I and *Eco*RV restriction sites are indicated and numbered accordingly. The *Bam*HI sites that flank the *erm* insertion are also indicated. The *Dra*I DNA fragment (**a**) that *erm*-specific probe DNA hybridised to is shown. The *Dra*I and *Eco*RV DNA fragments that probe DNA did not hybridise with is denoted by the grey dashed line and X.

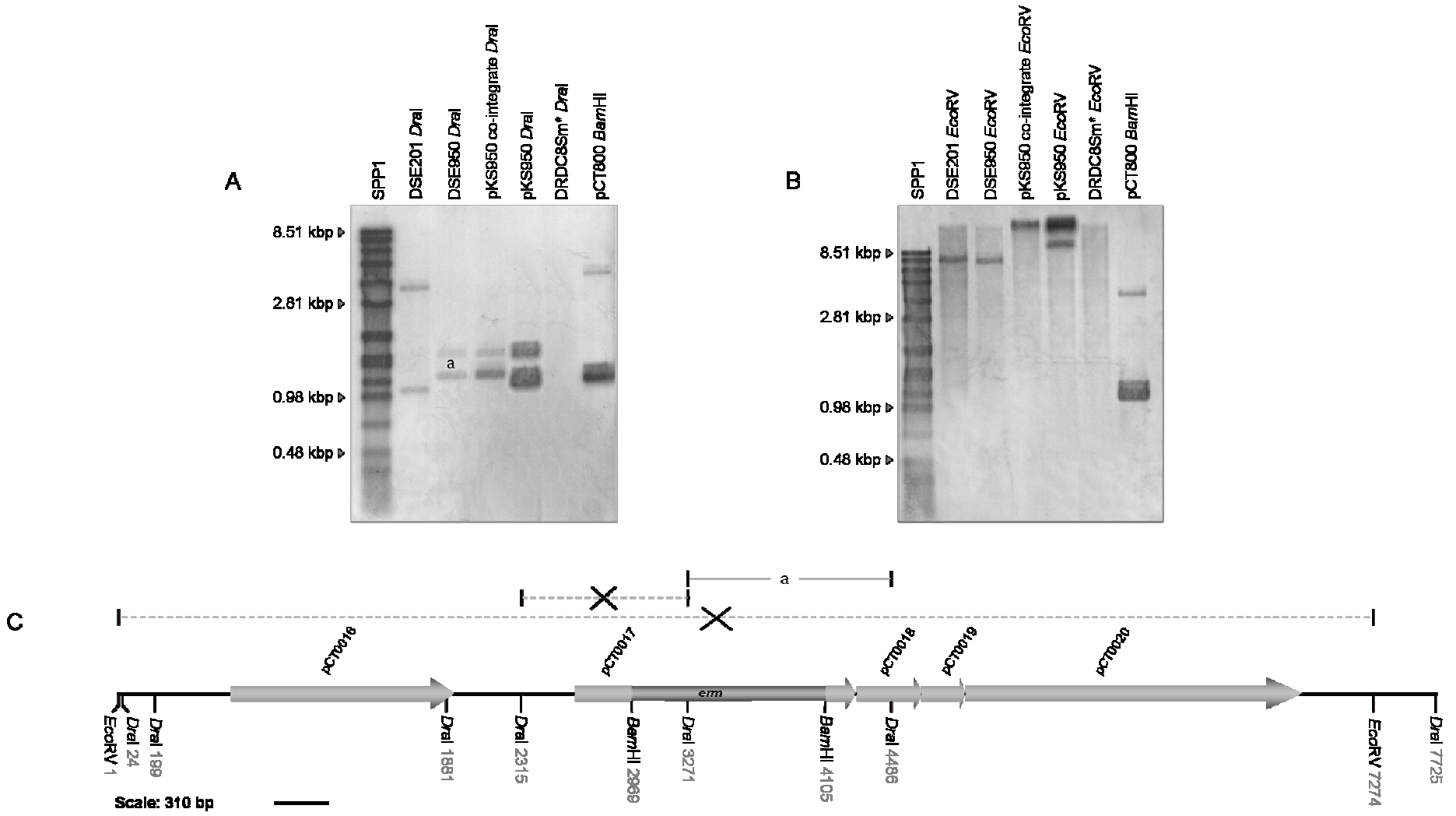
A
SPP1
DSE201 DraI
DSE950 DraI
pKS950 co-integrate DraI
pKS950 DraI
DRDC8Sm* DraI
pCT800 BamHI
8.51 kbp
2.81 kbp
0.98 kbp
0.48 kbp
a
B
SPP1
DSE201 EcoRV
DSE950 EcoRV
pKS950 co-integrate EcoRV
pKS950 EcoRV
DRDC8Sm* EcoRV
pCT800 BamHI
8.51 kbp
2.81 kbp
0.98 kbp
0.48 kbp
C
a
pCT0016
pCT0017
pCT0018
pCT0019
pCT0020
erm
EcoRV 1
DraI 24
DraI 189
DraI 1881
DraI 2315
BamHI 2869
DraI 3271
BamHI 4105
DraI 4486
EcoRV 7274
DraI 7725
Scale: 310 bp

Figure 4.8: PCR analysis of the putative mutant strains DSE951 and DSE952.

Panel A. Products **a** (1345 bp) and **b** (1162 bp) were amplified from DNA extracted from strain DSE951 using the FB1865/ermF2 and the p2037/ermR2 oligonucleotide pairs, respectively. Products **c** (1511 bp) and **d** (996 bp) were amplified from DNA extracted from strain DSE952 using the FB1865/ermF2 and the p2037/ermR2 oligonucleotide pairs, respectively. Amplicons were not produced from the no DNA negative (-ve) controls for either primer pair.

Panel B. PCR products **e** (645 bp) and **f** (2859 bp) were amplified from DNA extracted from strain DSE951 using the ermR/ermF and FB1865/p2037 oligonucleotide pairs, respectively. PCR products **g** (645 bp) and **h** (2859 bp) were amplified from DNA extracted from strain DSE952 using the ermR/ermF and FB1865/p2037 oligonucleotide pairs, respectively. A PCR product 1723 bp in size was amplified from the positive control strain DRDC8Sm* using the FB1865/p2037 oligonucleotide pair. Amplicons were not produced from the no DNA negative (-ve) controls for either primer pair.

Panel C. Diagrammatic representation of the theoretical *erm* insertion in ORF pCT0018 in strain DSE951. The relative position of oligonucleotide pairs specifically designed to amplify corresponding DNA fragments (products **a**, **b**, **e** and **f**) within this region are shown. The respective nucleotide sequence for each oligonucleotide is listed in Table 2.7.

Panel D. Diagrammatic representation of the theoretical *erm* insertion in ORF pCT0019 in strain DSE952. The relative position of oligonucleotide pairs specifically designed to amplify corresponding DNA fragments (products **c**, **d**, **g** and **h**) within this region are shown. The respective nucleotide sequence for each oligonucleotide is listed in Table 2.7.

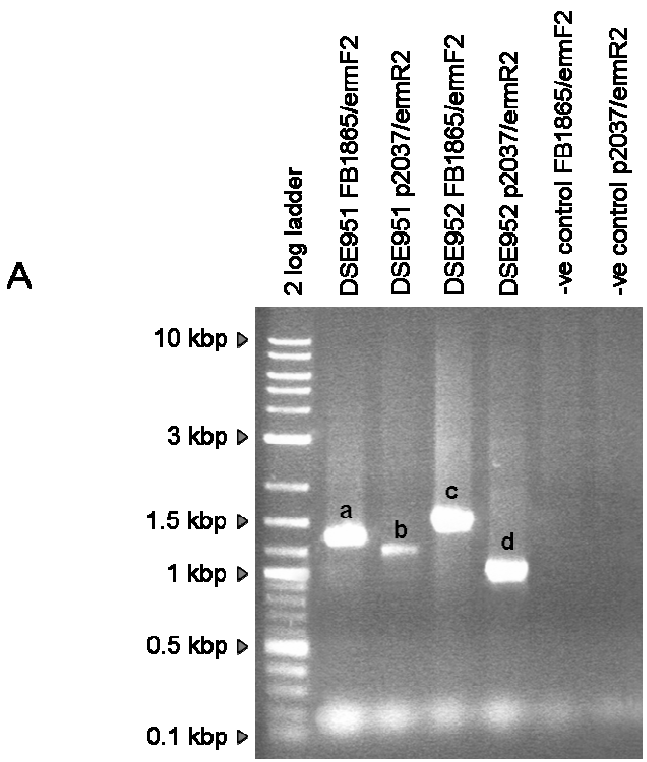

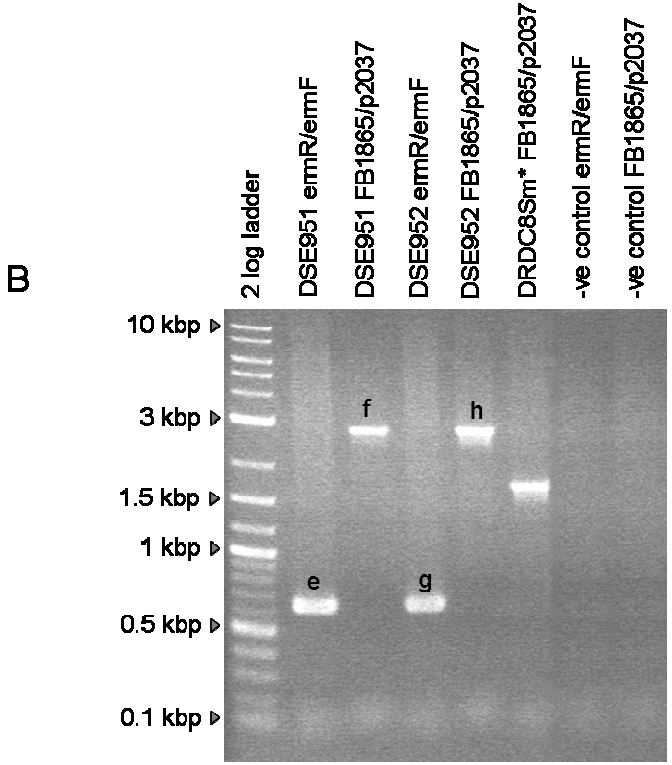

Figure continued next page……

Figure 4.8 continued